Smart Structures and Systems, *Vol. 15, No. 6 (2015) 1439-1461*
DOI: http://dx.doi.org/10.12989/sss.2015.15.6.1439

Seismic responses of base-isolated buildings: efficacy of equivalent linear modeling under near-fault earthquakes

Cenk Alhan* and Murat Özgür[a]

Department of civil Engineering, Istanbul University, 34320 Avcilar, Istanbul, Turkey

(Received September 3, 2013, Revised March 5, 2014, Accepted March 7, 2014)

Abstract. Design criteria, modeling rules, and analysis principles of seismic isolation systems have already found place in important building codes and standards such as the Uniform Building Code and ASCE/SEI 7-05. Although real behaviors of isolation systems composed of high damping or lead rubber bearings are nonlinear, equivalent linear models can be obtained using effective stiffness and damping which makes use of linear seismic analysis methods for seismic-isolated buildings possible. However, equivalent linear modeling and analysis may lead to errors in seismic response terms of multi-story buildings and thus need to be assessed comprehensively. This study investigates the accuracy of equivalent linear modeling via numerical experiments conducted on generic five-story three dimensional seismic-isolated buildings. A wide range of nonlinear isolation systems with different characteristics and their equivalent linear counterparts are subjected to historical earthquakes and isolation system displacements, top floor accelerations, story drifts, base shears, and torsional base moments are compared. Relations between the accuracy of the estimates of peak structural responses from equivalent linear models and typical characteristics of nonlinear isolation systems including effective period, rigid-body mode period, effective viscous damping ratio, and post-yield to pre-yield stiffness ratio are established. Influence of biaxial interaction and plan eccentricity are also examined.

Keywords: nonlinear isolation systems; equivalent linear modeling; effective stiffness; effective damping; base isolation; seismic isolation

1. Introduction

Seismic base isolation offers a reduction in the seismic energy input through use of laterally flexible bearings. The deformation is mostly concentrated at the isolation system placed underneath the super-structure which moves like a rigid body in case of an earthquake. This behavior, together with reduced seismic energy input, leads to reduced inter-story drifts and floor accelerations in seismic-isolated buildings compared to their fixed-base counterparts (Naeim and Kelly 1999). Among other references, Heaton *et al.* (1995), Kelly (1999), Liu (2005), York and Ryan (2008), Cardone *et al.* (2010), and Gueguen (2012) provide an insight on the important work done in the field of seismic isolation over the last two decades. Since the experimental and the actual observed behaviors of seismic-isolated buildings subjected to earthquake excitations have

*Corresponding author, Associate Professor, E-mail: cenkalhan@istanbul.edu.tr
[a] Former Graduate Student

http://www.techno-press.org/?journal=sss&subpage=8 ISSN: 1738-1584 (Print), 1738-1991 (Online)

proven the success of seismic base isolation in improving seismic performance significantly (Nagarajaiah and Xiaohong 2000, Sarrazin *et al.* 2005, Lakshmanan 2008, Tsai *et al.* 2010), the increasing popularity of the use of seismic isolation in many projects throughout the world comes at no surprise (Pan *et al.* 2005, Marioni 2009).

Important building codes and standards such as the Uniform Building Code (ICBO 1997) and the ASCE/SEI 7-05 standard (ASCE 2006) include chapters on seismic isolation which provide design criteria, modeling rules, and analysis principles of seismic-isolated structures. In order to be able to use the seismic analysis methods for seismic-isolated structures recommended by such codes, which are based on linear elastic theory (i.e., equivalent lateral response method, response spectrum method, and linear time history analysis method), the seismic isolators, which essentially exhibit nonlinear hysteretic behavior, have to be defined as equivalent linear elements with effective stiffness and effective (or equivalent) viscous damping properties. Effective stiffness is calculated at the design displacement and effective viscous damping is obtained using the area enclosed by the hysteresis loop.

Most of the previous research efforts on equivalent linear modeling and analysis concentrated on seismic-isolated bridge structures. Early work in this area includes studies by Turkington *et al*. (1989a, b), Hwang and Sheng (1993), Hwang *et al*. (1994), Hwang and Sheng (1994), Hwang (1996), and Hwang and Chiou (1996) in which various formulations of equivalent linear elastic properties of seismic isolation systems and their validity for use in modeling of seismic-isolated bridges are discussed. More recently, Franchin *et al*. (2001) raised concerns on the accuracy of equivalent linear models in capturing actual displacement and force responses of the isolation systems of seismic-isolated bridges. Subsequently, the equivalent damping equation presented in AASHTO (1999) was evaluated and an improved equivalent damping equation to obtain more reasonable estimates of the actual nonlinear response of seismic isolated bridges was suggested for far-fault earthquakes (Dicleli and Buddaram 2006) and near-fault earthquakes (Dicleli and Buddaram 2007a). Jara and Casas (2006) also proposed an equivalent damping ratio derived from the characteristics of bridges supported on lead rubber bearings (LRB) which improves the displacement prediction capability of the linear equivalent model.

There also exist recent studies that evaluate the accuracy of equivalent linear modeling and analysis for single-degree-of-freedom (SDOF) systems. Dicleli and Buddaram (2007b) evaluated the equivalent linear analysis procedure for seismic-isolated structures represented by SDOF systems and found that the characteristics of the ground motion and the characteristic strength of the isolator affect the accuracy of the equivalent linear analysis results for SDOF systems. Dall'Asta and Ragni (2008) discussed the formulation of equivalent linear modeling of nonlinear dynamic systems with high damping rubber bearing-based devices considering both transient and stationary behaviors. The effectiveness of the linear approximation in evaluating displacements and forces was determined via a parametric study on SDOF systems. Sayani and Ryan (2009) evaluated equivalent linear characterization of a nonlinear SDOF system with a rigid mass mounted on a single isolator in comparison to an alternative normalized strength characterization method.

All of the aforementioned studies consider SDOF systems or bridge structures which are idealized as rigid bodies. However, equivalent linear modeling is also used in the analysis of multi-story seismic-isolated structures and its efficacy may be different for the response of such structures. A first attempt in assessing the accuracy of equivalent linear modeling for the response of seismic-isolated models with flexible superstructures was presented by Matsagar and Jangid (2004) using a two-dimensional five-story shear frame structure. In a more recent study, Alhan and

Şahin (2011) investigated the influence of equivalent linear modeling of nonlinear isolation systems on the acceleration response of seismically isolated buildings and warned that significant errors in the calculation of floor accelerations may be introduced via such modeling.

While these studies provide very valuable first insight to the problem, there still exist other issues that were not considered explicitly before. Consequently, in this study we extend the work of Matsagar and Jangid (2004): (1) by taking into account a *three-dimensional* model under the influence of *bi-directional* ground excitation rather than a *two-dimensional* model under *uni-directional* ground excitation; (2) by taking into account *biaxial interaction* of isolators which may only be considered in a three-dimensional model and is particularly important when comparisons of equivalent linear models to nonlinear ones are studied since unlike actual nonlinear models, equivalent linear models of isolators can not take biaxial interaction into account; (3) by examining the efficacy of equivalent linear modeling in predicting *torsional base moments* which was not assessed by Matsagar and Jangid (2004) as it would only occur in *eccentric* three-dimensional models; and (4) in addition to other seismic response terms by also examining the efficacy of equivalent linear modeling in predicting *inter-story drifts* and *base shears* which were not reported by Matsagar and Jangid (2004). Furthermore, owing to a much *wider range* of nonlinear isolation systems with different characteristics used here as compared to those investigated by Matsagar and Jangid (2004), it was possible in the current study to portray the *variation of the accuracy* of the estimates of peak structural responses from equivalent linear models with respect to effective period, rigid-body mode period, effective viscous damping ratio, and post-yield to pre-yield stiffness ratio, which were not reported by Matsagar and Jangid (2004).

2. Mathematical modeling

A seismic-isolated structure is formed by an isolation system composed of isolators, a base floor that connects all elements of the isolation system, and a superstructure that is supported by the isolation system. In this study, a generic three dimensional seismic-isolated shear structure, which is shown in Fig. 1, is used in the numerical experiments (Özgür 2010).

A generic shear building model representing a class of buildings with a given natural period and distribution of stiffness over the height can be used to obtain accurate seismic response quantities of both the isolation systems and the superstructures of that class of seismic isolated buildings (Alhan and Sürmeli 2011). Including the base floor, the generic building of this study consists of a total number of six floors.

The model structure is analyzed using 3DBASIS, which is an academic software developed by Nagarajaiah *et al*. (1991) for the linear and nonlinear modeling and analysis of three dimensional base isolated structures. The equations of motion of a seismic-isolated shear structure subjected to earthquake excitation, the numerical solution method used, and the verification of 3DBASIS are explained and discussed in detail by Nagarajaiah *et al*. (1991).

2.1 Superstructure and base

All floor masses and all story stiffnesses are considered to be equal. All floors are assumed to be fully rigid and all floor masses are lumped at the center of mass of each floor. The centers of mass of the floors lie on the same vertical axis. There are three degrees of freedom per floor: one for each translational direction and one for rotational. The story stiffnesses are adjusted to provide

fundamental fixed-base periods of 0.5 s in both translational directions and a rotational period of 0.3 s. Superstructure modal damping ratios are considered to be 5% and constant for all modes. The superstructure is assumed to remain linear elastic.

A rigid base floor connects all isolators which form the isolation system as shown in Fig. 1. The mass of the base is equal to the mass of an i^{th} floor of the superstructure. The mass of the base is lumped at the center of mass of base which lies on the same vertical axis with the floors of the superstructure. Including the three degrees of freedom for the base (two translational and one rotational), there exist a total of 18 degrees of freedom in the seismic-isolated structure.

2.2 Isolation system

Nonlinear isolation systems considered in this study are composed of elastomeric-based isolators and therefore the actual nonlinear force-deformation behavior of the isolation systems is hysteretic. The hysteresis loop can be represented by a bi-linear model which comprises of two branches whose slopes are named as the pre-yield (initial or elastic) stiffness (K_1) and the post-yield (plastic) stiffness (K_2). In the following subsections, first, the modeling and properties of the nonlinear isolation systems and then, the modeling and properties of the equivalent linear isolation systems are described.

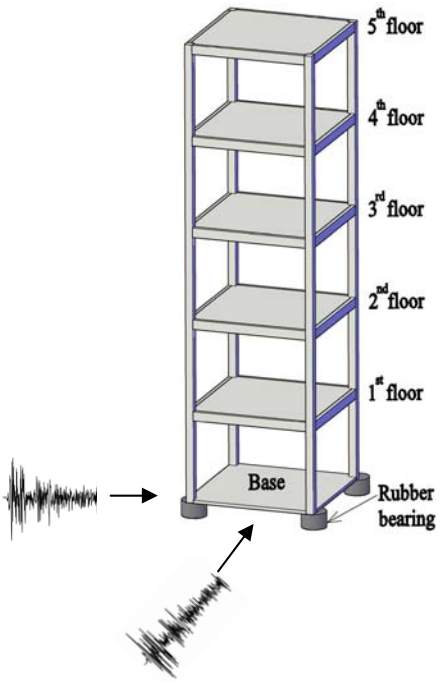

Fig. 1 Generic five story shear structure

2.2.1 Nonlinear models

Among the important properties of nonlinear isolation systems are the rigid-body mode period (or the isolation period), T_0 and the yield level, Q/W, where Q is the characteristic strength and W is the total weight of the structure. The rigid-body mode period based on the post-yield stiffness is given by

$$T_0 = \frac{2\pi}{\omega_0} \tag{1}$$

where ω_0 is the post-yield angular frequency given by

$$\omega_0 = \sqrt{\frac{K_2}{M}} \tag{2}$$

where K_2 is the post-yield stiffness and M is the total mass of the structure (Nagarajaiah et al 1991). The relation between the pre-yield stiffness (K_1) and the post-yield stiffness (K_2) of an isolation system with a yield displacement D_y is given by (Naeim and Kelly 1999)

$$K_1 = \frac{Q}{D_y} + K_2 \tag{3}$$

Pre-yield stiffness (K_1) depends on yield displacement and yield strength (F_y) of the isolation system

$$K_1 = \frac{F_y}{D_y} \tag{4}$$

In order to cover a wide range, 21 different isolation systems with different isolation periods (T_0) and yield levels (Q/W) are considered. Rigid-body mode isolation periods of T_0 = 2.00 s, 2.25 s, 2.50 s, 2.75 s, 3.00 s, 3.25 s, and 3.50 s and yield levels of Q/W = 5%, 7.5%, and 10% and combinations thereof are included in the investigation. Table 1 lists the properties of the isolation systems calculated using Eqs. (1)-(4). Included in Table 1 are the post-yield to pre-yield stiffness ratios of all isolation systems represented by α.

Table 1 Properties of the isolation systems

		Q / W=5%			**Q / W=7.5%**			**Q / W=10%**		
T_0	**K_2 / W**	**K_1 / W**	**α**	**F_y / W**	**K_1 / W**	**α**	**F_y / W**	**K_1 / W**	**α**	**F_y /W**
(s)	(1/m)	(1/m)	(-)	(-)	(1/m)	(-)	(-)	(1/m)	(-)	(-)
2.00	1.006	3.506	0.287	0.070	4.756	0.212	0.095	6.006	0.168	0.120
2.25	0.795	3.295	0.241	0.066	4.545	0.175	0.091	5.795	0.137	0.116
2.50	0.644	3.144	0.205	0.063	4.394	0.147	0.088	5.644	0.114	0.113
2.75	0.532	3.032	0.175	0.061	4.282	0.124	0.086	5.532	0.096	0.111
3.00	0.447	2.947	0.152	0.059	4.197	0.107	0.084	5.447	0.082	0.109
3.25	0.381	2.881	0.132	0.058	4.131	0.092	0.083	5.381	0.071	0.108
3.50	0.329	2.829	0.116	0.057	4.079	0.081	0.082	5.329	0.062	0.107

2.2.2 Equivalent linear models

In order to investigate the effect of equivalent linear modeling on the seismic response in a comparative fashion, the nonlinear seismic isolation systems described above have to be defined as equivalent linear systems with effective stiffnesses (K_{eff}) and effective viscous damping ratios (β_{eff}). The necessary steps to construct an equivalent linear model are as follows (Matsagar and Jangid 2004): First, the total effective stiffness of a nonlinear isolation system with a characteristic force Q and a peak isolation system displacement, D is calculated as

$$K_{eff} = K_2 + \frac{Q}{D} \tag{5}$$

Then, the effective isolation period and the effective angular frequency then given by

$$T_{eff} = 2\pi\sqrt{\frac{M}{K_{eff}}} \tag{6}$$

$$\omega_{eff} = \sqrt{\frac{K_{eff}}{M}} \tag{7}$$

Finally, effective viscous damping is obtained using the area enclosed by the hysteresis loop. Accordingly effective viscous damping ratio of an isolation system with a yield displacement D_y is

$$\beta_{eff} = \frac{4Q(D-D_y)}{2\pi K_{eff} D^2} \tag{8}$$

Using Eqs. (7) and (8), the total effective viscous damping constant required for the modeling of linear isolation systems composed of linear isolation elements can be calculated by

$$C_{eff} = 2M\omega_{eff}\beta_{eff} \tag{9}$$

3. Earthquake data

Since seismically isolated buildings are specifically challenged by near-fault earthquakes (Heaton *et al.* 1995) the historical earthquake records used in this study are selected to represent near-fault earthquakes which were used previously by Kalkan and Kunnath (2006) as representatives of near-fault earthquakes. The names, recording stations, occurrence dates, closest distances to fault, moment magnitudes, peak ground accelerations (PGA), peak ground velocities (PGV), and peak ground displacements (PGD) of the earthquake records are summarized in Table 2. For use in the plots and tables throughout this paper, each record is also given a label as reported in Table 2. The 10% damped spectral acceleration plots of the the earthquakes are given in Fig. 2. All data regarding the earthquakes are retrieved from the Peer Strong Motion Databank (PEER 2000).

Table 2 Earthquake Records

Name	Label	Recording Station	Label	Date	Closest Distance to Fault (km)	M_w	PGA (g)	PGV (cm/s)	PGD (cm)
Cape Mendocino	PET090	Petrolia	PET	25/04/1992	9.5	7.1	0.66	90.16	28.89
Northridge	SYL360	Sylmar Olive View	SYL	17/01/1994	6.4	6.7	0.84	129.6	32.7
Loma Prieta	LGP000	LGPC	LGP	18/10/1989	6.1	6.9	0.56	94.8	41.2
Kobe	KJM000	KJMA	KJM	16/01/1995	0.6	6.9	0.82	81.3	17.7

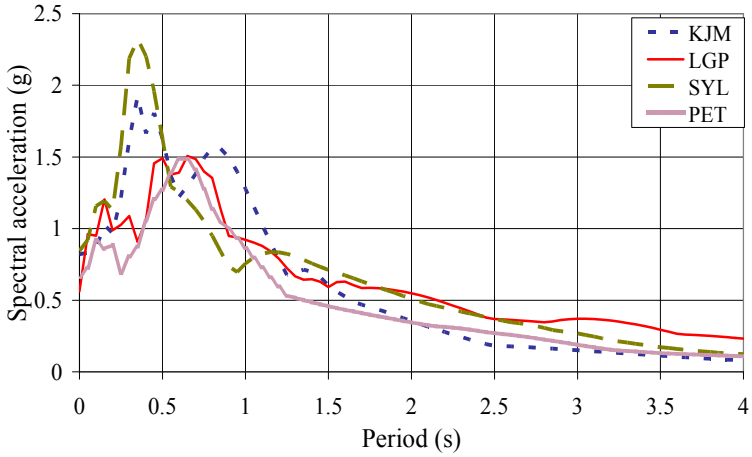

Fig. 2 Acceleration response spectra (10% damped)

4. Simulations and assessment criteria

4.1 Construction of equivalent linear models

The models with nonlinear isolation systems listed in Table 1 are subjected uni-directional earthquake loadings as shown in Fig. 3(a). For this set of analysis, models with no plan eccentricity in which the centers of mass coincide with centers of rigidity, are subjected to earthquakes listed in Table 2. As a result, peak isolation system displacements of the nonlinear isolation systems (D), which are required for the construction of equivalent linear models (Eqs. (5)-(9)), are obtained and presented in Table 3. The total effective stiffnesses and the total viscous damping constants of the equivalent linear isolation systems are calculated via Eqs. (5) and (9), respectively.

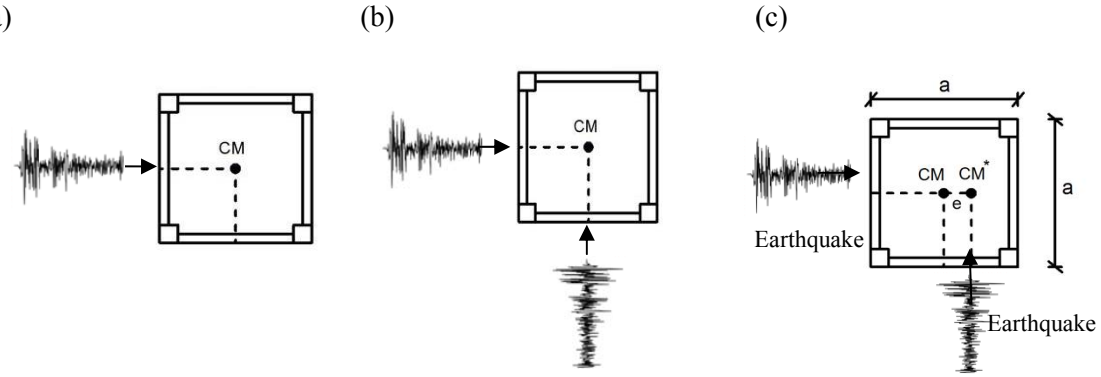

Fig. 3 Earthquake loading: (a) uni-directional with no plan eccentricity, (b) bi-directional with no plan eccentricity, and (c) bi-directional with 5% eccentricity (e=0.05a) and 10% eccentricity (e=0.10a)

Table 3 Nonlinear peak isolation system displacements and [spectral displacements]*

Yield level Q / W (%)	Isolation period T_0 (s)	Peak isolation system displacement (cm)			
		KJM	PET	SYL	LGP
5	2.00	33.14 [36.88]*	30.91 [31.69]	56.99 [59.52]	50.68 [58.26]
	2.25	32.30 [33.57]	33.28 [33.54]	57.02 [59.93]	53.83 [61.89]
	2.50	30.50 [29.52]	35.94 [37.16]	59.47 [59.21]	51.93 [60.01]
	2.75	27.60 [25.14]	36.90 [37.84]	59.27 [60.21]	54.33 [58.88]
	3.00	27.72 [24.40]	37.86 [37.49]	58.41 [58.36]	63.44 [65.77]
	3.25	29.08 [25.48]	38.94 [35.90]	57.53 [54.35]	75.64 [83.19]
	3.50	29.73 [25.52]	39.82 [33.47]	55.72 [51.36]	79.53 [88.37]
7.5	2.00	28.21 [31.73]	29.01 [28.80]	47.13 [49.62]	44.13 [49.81]
	2.25	26.69 [29.00]	31.33 [30.51]	47.87 [50.49]	45.93 [53.11]
	2.50	25.36 [26.33]	33.13 [31.32]	48.88 [51.11]	44.32 [51.31]
	2.75	23.93 [23.66]	34.59 [31.52]	49.45 [50.85]	40.32 [45.97]
	3.00	22.87 [21.34]	35.72 [31.21]	49.61 [49.72]	44.19 [50.64]
	3.25	21.85 [19.45]	36.74 [31.22]	49.39 [48.06]	47.83 [54.60]
	3.50	21.15 [18.76]	37.51 [31.38]	48.95 [46.09]	50.80 [57.07]
10	2.00	22.91 [24.99]	26.82 [26.23]	42.00 [44.63]	37.86 [41.78]
	2.25	21.39 [23.43]	29.02 [27.76]	42.58 [44.83]	40.32 [45.14]
	2.50	19.94 [21.68]	30.71 [28.56]	42.77 [44.42]	39.46 [43.85]
	2.75	18.62 [20.13]	32.07 [28.84]	42.57 [43.80]	36.57 [39.74]
	3.00	18.06 [18.97]	33.18 [28.80]	42.16 [42.76]	37.23 [40.44]
	3.25	17.99 [18.06]	34.07 [28.89]	41.65 [41.52]	39.80 [43.44]
	3.50	18.08 [17.31]	34.83 [28.83]	41.24 [40.15]	42.02 [45.84]

* Values given in brackets are the spectral displacements obtained for the effective period and the effective damping ratio that are associated with the corresponding nonlinear isolation system.

Effective periods (Eq. (7)) and effective damping ratios (Eq. (9)) of the equivalent counterparts of the nonlinear isolation systems are depicted as a scatter plot in Fig. 4. As it can be seen from the figure, a very wide range of effective periods (T_{eff} = 1.67 s ~ 3.21 s) and effective damping ratios (β_{eff} = 5% ~ 36%) -corresponding to a total of 84 equivalent linear isolation systems- are taken into account.

It is well known that an earthquake displacement spectrum can be used to obtain the peak displacement of a linear elastic single degree of freedom system with a certain natural period and damping ratio. Since the superstructure of a seismically isolated building typically behave like a rigid-body, the nonlinear peak isolation system displacement under an earthquake excitation should then be close to the spectral displacement for the effective period and effective damping ratio that are associated with that nonlinear isolation system. This fact is used for validation purposes in this study: spectral displacements are obtained for the effective period and the effective damping ratio that are associated with each nonlinear system and given in Table 3 in brackets along with the actual nonlinear peak isolation system displacements. It is shown that the differences are less than about 15%, only.

4.2 Structural response parameters

Peak isolation system displacements (d), peak top floor accelerations (a), peak first story drifts (Δ), peak base shears (V), and peak torsional base moments (M) are included in this investigation. These structural response parameters are calculated for models equipped with both nonlinear and corresponding equivalent linear isolation systems. Subscript N (i.e., d_N, a_N, Δ_N, V_N, M_N) and L (i.e., d_L, a_L, Δ_L, V_L, M_L) are used in cases of nonlinear and equivalent linear isolation systems, respectively.

In order to examine the effects of uni-directional loading, bi-directional loading, and plan eccentricity on the efficacy of equivalent linear modeling, all structural response parameters are calculated for four different cases as shown in Fig. 3. First set of analysis is conducted for uni-directional earthquake loading with no plan eccentricity (Fig. 3(a)). Second set of analysis is conducted for bi-directional earthquake loading with no plan eccentricity (Fig. 3(b)). Third and fourth set of analysis are conducted for bi-directional loading with 5% and 10% plan eccentricities (Fig. 3(c)). In order to introduce e = 5 % and e = 10 % eccentricity in the models, the centers of floor masses (CM) which coincide with the centers of floor rigidities for e = 0% case are shifted by 5% and 10% of the floor plan dimensions (CM*) as shown in Fig. 3(c), respectively. It should be noted here that although sliding PTFE devices may be used in the design of an isolation system in order to minimize torsional effects, here eccentric cases are intentionally created since part of the objectives of this study is to assess the efficacy of equivalent linear modeling in predicting torsional base moments. Furthermore, a 5% eccentricity corresponds to the accidental eccentricity case which has to be taken into account regardless of the composition of the isolation system.

For use in the figures, shorthand symbols are introduced here. **U** and **B** stand for **U**nidirectional and **B**idirectional earthquake loadings, respectively. **e5** and **e10** stand for plan eccentricities of **e = 5%** and **e = 10 %**, respectively. When there exists no eccentricity, **e** is not included in the shorthand symbol. **QW5**, **QW7.5**, and **QW10** stand for yield levels of **Q/W = %5**, **%7.5**, and **%10**, respectively. For example **BQW7.5e5** represents the structural model with a 5% plan eccentricity supported by an isolation system with a yield level of Q/W = 7.5% subjected to a bidirectional earthquake loading (and **BQW7.5** corresponds to noneccentric case).

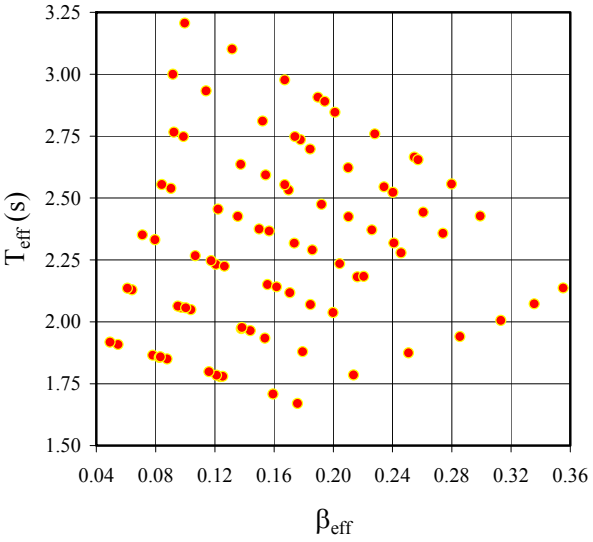

Fig. 4 Scatter of effective viscous damping ratio and effective period

4.3 Dispersion and average absolute percent error

In order to quantify the efficacy of the equivalent linear modeling in predicting the seismic response terms of multi-story structures with nonlinear seismic-isolation systems, the dispersion, D_r of the **L**inear/**N**onlinear ratio of each seismic response term, i.e., peak isolation system displacement, peak top floor acceleration, peak first story drift, peak base shear, and peak torsional base moment, – generically represented here by r – with respect to 1.0 is calculated by the dispersion equation given by (Chapra and Raymond 2002)

$$D_r = \left| \frac{(r_L / r_N) - 1.0}{(r_L / r_N)} \right| \tag{10}$$

It should be noted here that, for $r_L / r_N = 1.0$, i.e., a perfect estimation of the actual nonlinear response by the equivalent linear modeling, the dispersion is equal to 0.0. On the other hand, dispersion values larger than 1.0 correspond to cases for which $r_N > 2r_L$, i.e., equivalent linear modeling produces highly unconservative estimates of the actual nonlinear response (Dicleli and Buddaram 2007a).

As another quantification method, which was also used by Dicleli and Buddaram (2007b), the absolute percent deviation from $r_L / r_N = 1.0$ is calculated for each response term r and averaged for n cases in order to obtain the average asolute percent error, e_r (Kottegoda and Rosso 1997)

$$e_r = \sum_{1}^{n} \frac{|r_L / r_N - 1.0|}{n} \times 100 \tag{11}$$

5. Discussion of results

The variations of the linear to nonlinear ratios of structural response parameters for all models with respect to the rigid-body mode period (T_0) are given in Figs. 5-8 for peak isolation system displacements, peak top floor accelerations, peak first story drifts, peak base shears, and peak torsional base moments represented by d_L/d_N, a_L/a_N, Δ_L/Δ_N, and V_L/V_N, respectively. Included in these figures are the results for both uni-directional and bi-directional loading cases under KJM, SYL, PET, and LGP earthquakes, seperately. For visual convenience, a solid line is drawn at 1.0 in each plot, representing a perfect estimate of the actual nonlinear response by the equivalent linear model. Results below and above this line corresponds to unconservative and conservative estimates of the equivalent linear modeling, respectively. It is seen from these figures that there exists a dependence on the earthquake loading as the response ratios obtained for the same models differ quantitatively for different earthquakes. The efficacy of the equivalent linear modeling also vary with respect to the specific characteristics (Q/W ratio and T_0) of the nonlinear isolation systems.

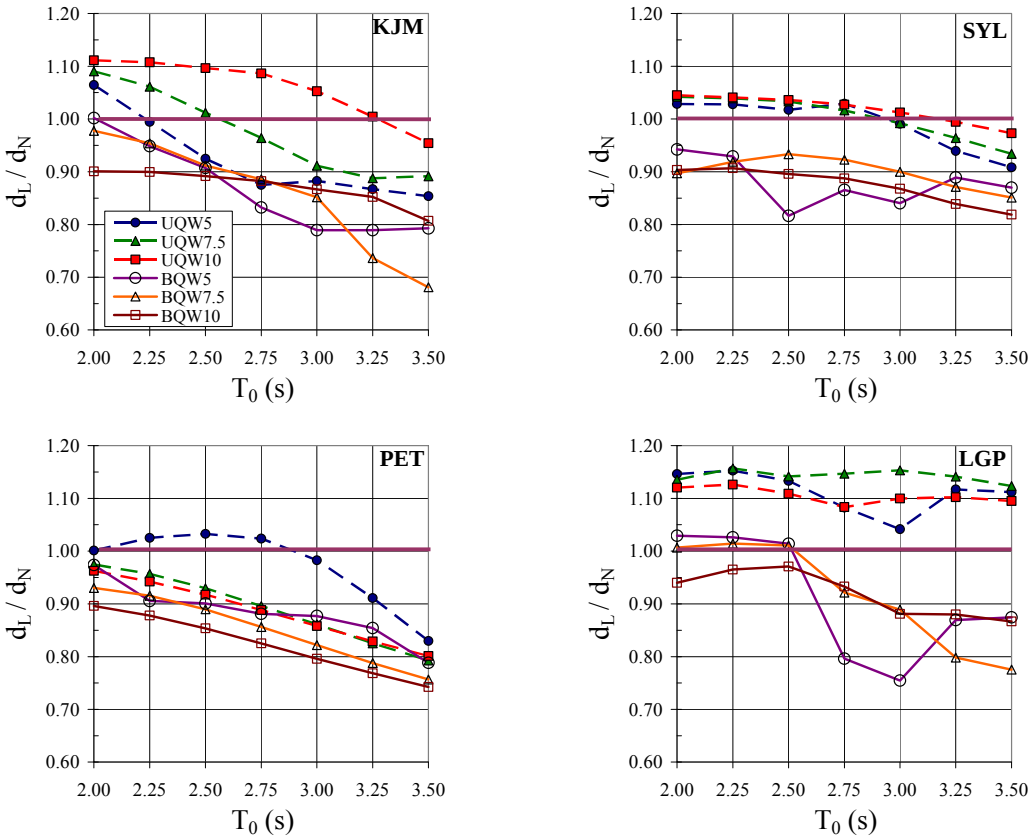

Fig. 5 Variation of the ratio of peak isolation system displacement from equivalent linear model, d_L, to that obtained by actual nonlinear model, d_N, with respect to the rigid-body mode period, T_0

Another important finding obtained from these figures is that the linear/nonlinear response ratios obtained for uni-directional and bi-directional loading cases differ. The difference is particularly large in case of peak base displacement ratios. Since the biaxial interaction occurs between the isolators at the isolation level, its effect would naturally be more prominent on the isolation system displacements and less on the rest of the structural parameters. The reader here is reminded that biaxial interaction can only be taken into account in case of nonlinear modeling. In case of equivalent linear models, isolation elements in perpendicular directions behave independently.

Fig. 5 shows that the d_L/d_N ratios for bi-directional loadings are consistently below those for uni-directional loading. Furthermore, while most d_L/d_N ratios stay above 1.0 line for uni-directional loading, they are below 1.0 line for bi-directional loading cases. This has an important effect since it reverses the conclusions on the conservativeness of equivalent linear modeling in estimating the actual peak displacement responses of nonlinear models previously reached by Matsagar and Jangid (2004). In that study, Matsagar and Jangid (2004) had concluded that equivalent linear modeling mostly overpredicts peak displacement responses ($d_L/d_N > 1.0$). However, they used a two dimensional structural model and a uni-directional loading in their study and thus neglected the effect of biaxial interaction. However, using a three dimensional model with bi-directional loading, which is more realistic, and owing to the effect of biaxial interaction effect, we observe here that in fact equivalent linear modeling mostly produce unconservative estimates of peak displacement responses ($d_L/d_N < 1.0$).

Although differences are observed between the linear/nonlinear response ratios for bi-directional and uni-directional loadings, unlike peak base displacements, there exist no consistent relationship between the linear/nonlinear response ratios for bi-directional and uni-directional loading cases in terms of peak top flor accelerations, peak first story drifts, and peak base shears (Figs. 6-8). Linear/nonlinear response ratios may be either smaller or larger for bi-directional loading compared to uni-directional loading depending on the type of the isolation system.

Next, the effect of plan eccentricity on the efficacy of the equivalent linear modeling in predicting torsional base moments is investigated by repeating all bi-directional analyses for e = 5 % and e = 10% eccentricity cases (Fig. 3(c)). Fig. 9 depicts the effect of eccentricity on the M_L/M_N ratios. As it can be seen from Fig. 9 the M_L/M_N ratios can be as low 0.40, showing a significant underestimation of the actual response by the equivalent linear modeling.

The variations of the Linear to Nonlinear ratios of structural response parameters with respect to the effective period (T_{eff}) and effective viscous damping ratio (β_{eff}) are given in Fig. 10 for the non-eccentric case. Included in these figures are the results for bi-directional loading cases under KJM, SYL, PET, and LGP earthquakes, seperately. While these plots portray the clear dependency of Linear/Nonlinear ratios on the effective period and effective damping, potential trends depending on increasing T_{eff} and β_{eff} are discussed via dispersion plots, which are presented next. Regardless of the earthquake type, it is seen that the equivalent linear modeling produce unconservative estimates of peak base displacements and peak torsional base moments (i.e., $d_L/d_N < 1.0$ and $M_L/M_N < 1.0$) and conservative estimates of peak top floor accelerations, peak first story drift ratios and peak base shears (i.e., $a_L/a_N > 1.0$, $\Delta_L/\Delta_N > 1.0$, and $V_L/V_N > 1.0$). Of the unconservative estimates, while M_L/M_N values can be distinctly low (up to 0.40), d_L/d_N values stay approximately within 0.8 to 1.0 band. The average values for d_L/d_N and M_L/M_N are 0.88 and 0.68, respectively. Of the conservative estimates, while Δ_L/Δ_N, and V_L/V_N values are close to each other and can be distinctly high (up to 1.80), a_L/a_N values stay approximately within 1.0 to 1.4 band. The average values for a_L/a_N, Δ_L/Δ_N, and V_L/V_N are 1.11, 1.12, and 1.09, respectively.

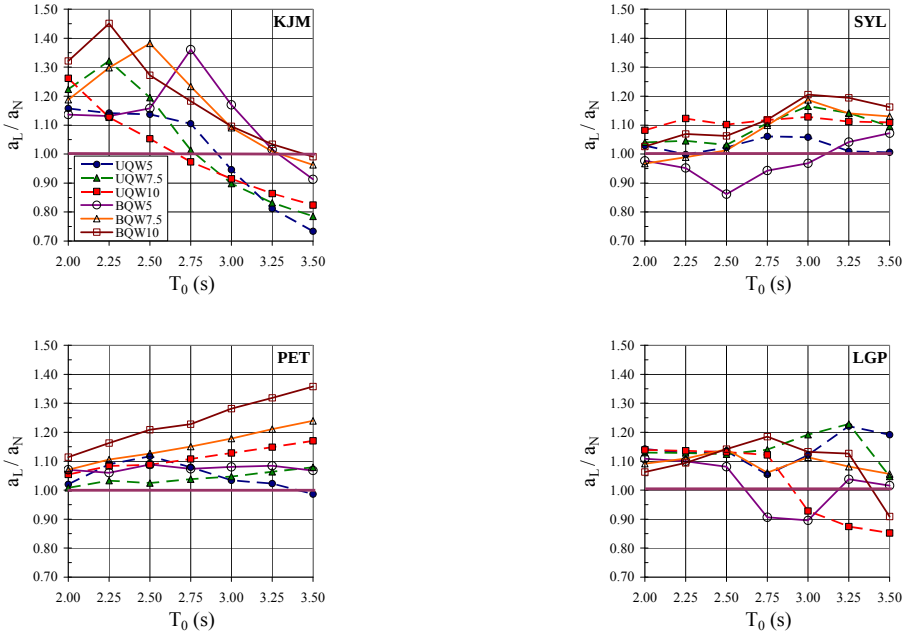

Fig. 6 Variation of the ratio of peak top floor acceleration from equivalent linear model, a_L, to that obtained by actual nonlinear model, a_N, with respect to the rigid-body mode period, T_0

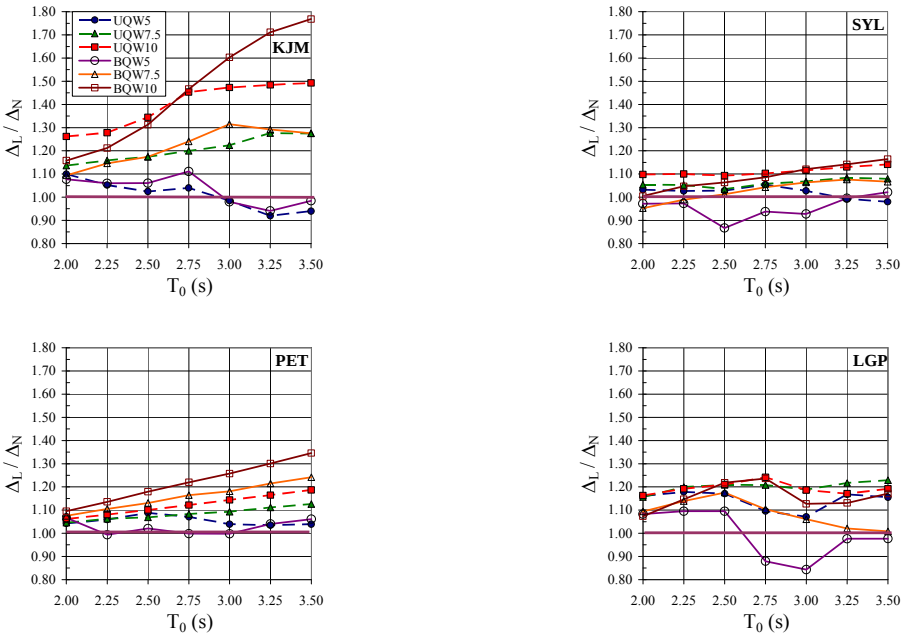

Fig. 7 Variation of the ratio of peak first story drift from equivalent linear model, Δ_L, to that obtained by actual nonlinear model, Δ_N, with respect to the rigid-body mode period, T_0

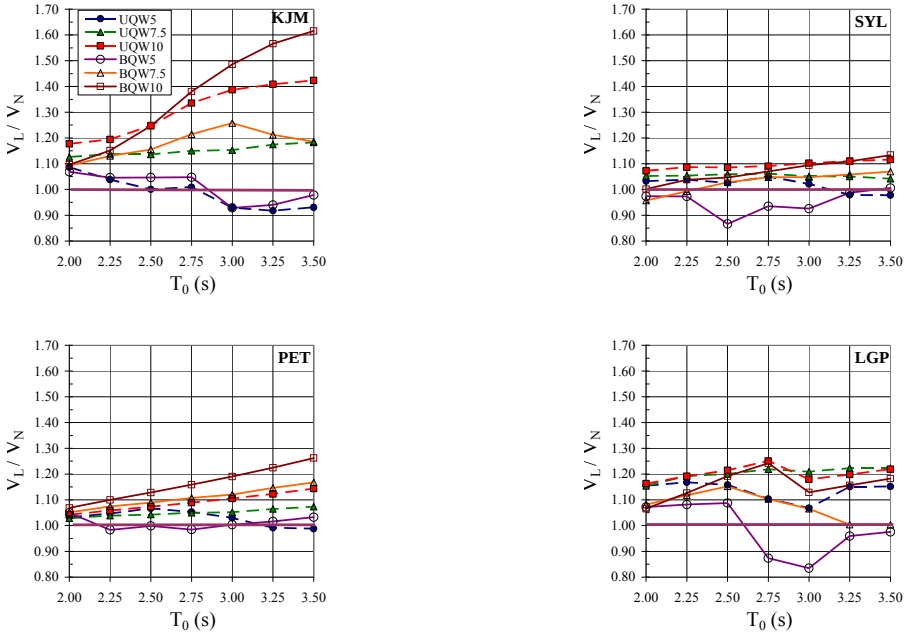

Fig. 8 Variation of the ratio of peak base shear from equivalent linear model, V_L, to that obtained by actual nonlinear model, V_N, with respect to the rigid-body mode period, T_0

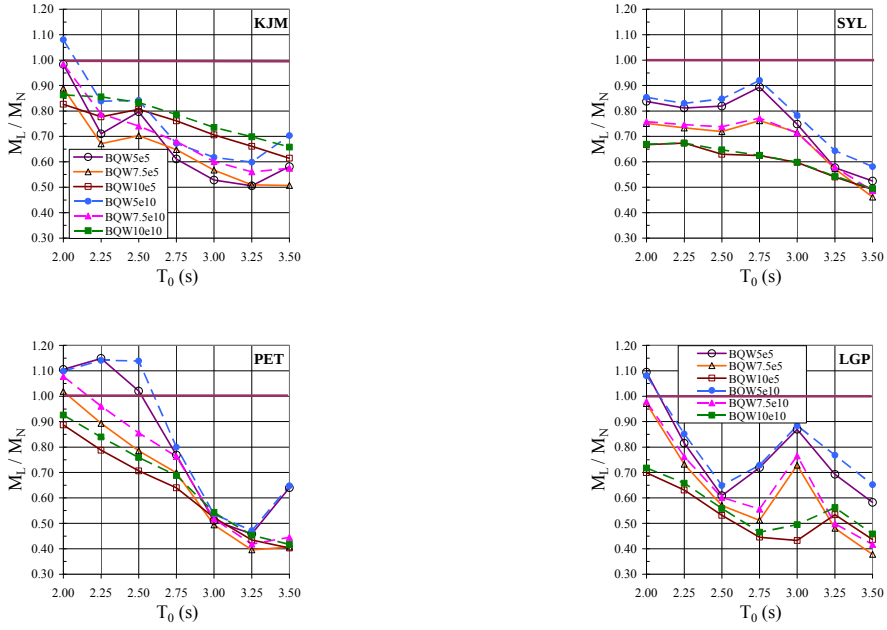

Fig. 9 Variation of the ratio of peak torsional base moment obtained by equivalent linear model, M_L, to that obtained by actual nonlinear model, M_N, with respect to the rigid-body mode period, T_0

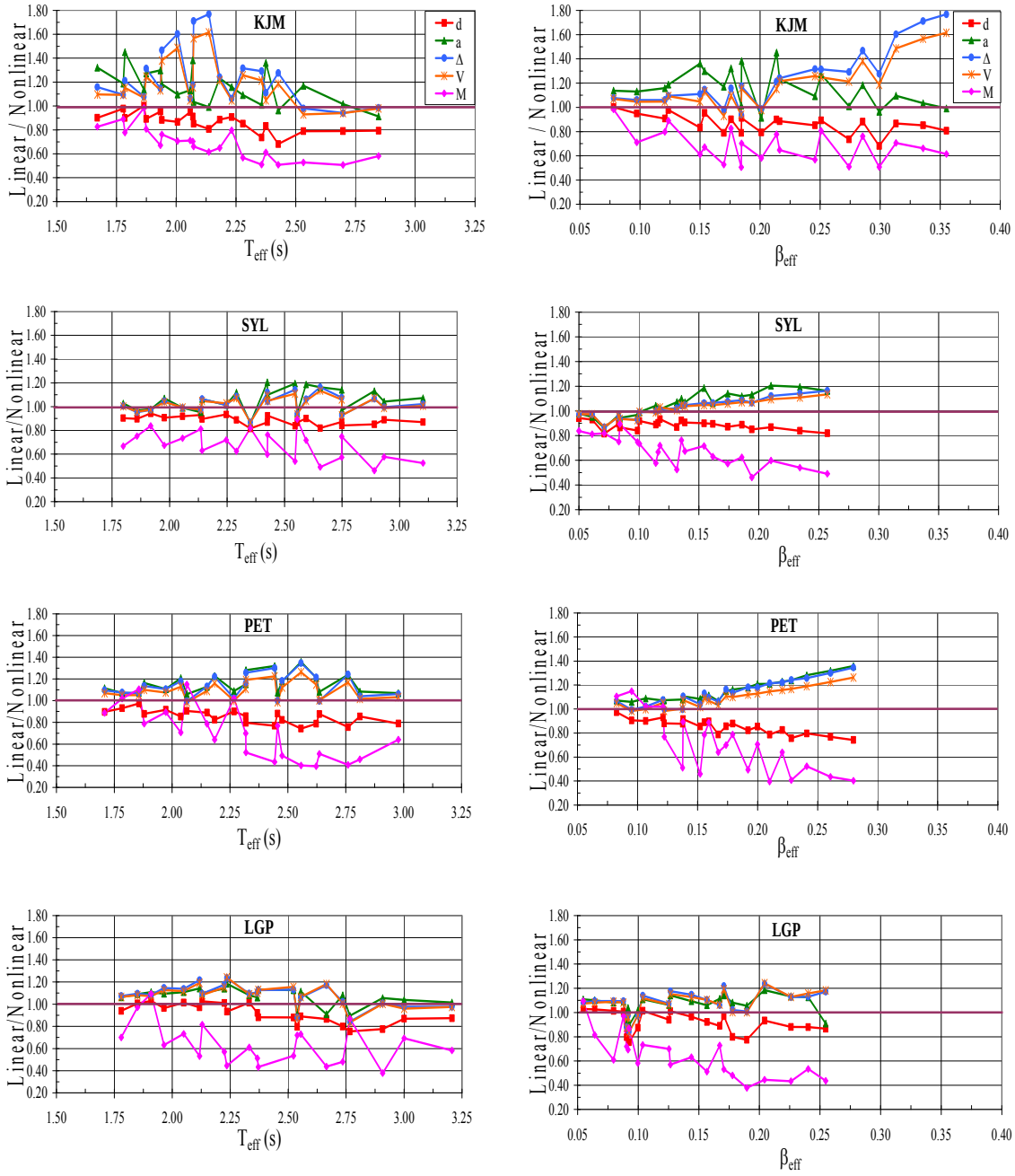

Fig. 10 Variations of the ratios of peak structural responses obtained by equivalent linear models to those obtained by nonlinear models with respect to effective period (T_{eff}) and effective viscous damping ratio (β_{eff})

D_d, D_a, D_Δ, D_V, and D_M, which represent dispersions of d_L/d_N, a_L/a_N, Δ_L/Δ_N, V_L/V_N, and M_L/M_N with respect to 1.0, respectively, are calculated by Eq. (10) and plotted with respect to rigid-body mode period, T_0 (Fig. 11). While most of the dispersion data for D_d, D_a, D_Δ, and D_V are below 0.25, showing a small to moderate dispersion from Linear/Nonlinear = 1.0 ratio, D_M values are rather high (go up to 1.75). As discussed above, most of this dispersion data are associated with unconservative estimates of peak base displacements and peak base torsional moments and conservative estimates of peak top floor accelerations, peak first story drift ratios, and peak base shears. Trendlines are also fitted to data in order to examine trends with respect to T_0. While exponential fits were suitable for D_d and D_M data, linear fits were suitable for others. It is observed that while D_d and D_M increase rapidly (with an increasing rate) as the rigid-body mode period increases, D_a, D_Δ, and D_V stays almost constant. Therefore, it can be concluded that equivalent linear models produce much better estimates of peak base displacements and peak torsional base moments for seismic-isolation systems with smaller rigid-body mode periods. However, there exists no clear relation between the rigid-body mode period and the accuracy of the estimates of other structural response parameters.

In order to examine the variation of dispersion values with respect to the effective period and see if there exist any trends, D_d, D_a, D_Δ, D_V, and D_M versus T_{eff} plots are given in Fig. 12. While logarithmic fits were suitable for D_d and D_M data since both increase with a decreasing rate as the effective period increases, no clear trends were observed for D_a, D_Δ, and D_V data as they were scattered widely with no clear dependence on Teff. Therefore, it can be concluded that equivalent linear models produce better estimates of peak base displacements and peak torsional base moments for seismic-isolation systems with smaller effective periods. However, there exists no clear relation between the effective period and the accuracy of the estimates of other structural response parameters.

The variations of dispersion values with respect to the effective viscous damping ratio, β_{eff}, are plotted and given in Fig. 13 for D_d, D_a, D_Δ, D_V, and D_M. Exponential fits were suitable for all dispersion data. Therefore, it is concluded that equivalent linear models produce better estimates of peak base displacements, peak top floor accelerations, peak first story drift ratios, peak base shears, and peak torsional base moments for seismic-isolation systems with smaller effective viscous damping ratios.

The variations of dispersion values with respect to the post-yield to the pre-yield stiffness ratio, α, are plotted and given in Fig. 14 for D_d, D_a, D_Δ, D_V, and D_M. It is seen that the efficacy of linear analysis and modeling increase with increasing α in terms of all response parameters. This would be an expected behavior since the nonlinearity of the isolation system increases with decreasing α. While exponential fits were suitable for D_d and D_M data, linear fits were suitable for others. Therefore, it can be concluded that equivalent linear models produce better estimates of peak top floor accelerations, peak first story drifts, and peak base shears and much better estimates of peak base displacements and peak torsional base moments for seismic-isolation systems with bigger post-yield to pre-yield stiffness ratios.

The average absolute percent errors for peak base displacement (e_d), peak top floor acceleration (e_a), peak first story drift ratio (e_Δ), peak base shear (e_V), and peak torsional base moment (e_M) are calculated by Eq. (11) and shown in Fig. 15. Except for peak base moments, the average absolute percent errors for structural responses are moderate. Of these, while the smallest is for peak base shear (e_V=11.4%), the largest is for peak first drift ratio (e_Δ=13.8%). On the other hand, the average absolute errors are significantly high for peak base moments (e_M=63.7%).

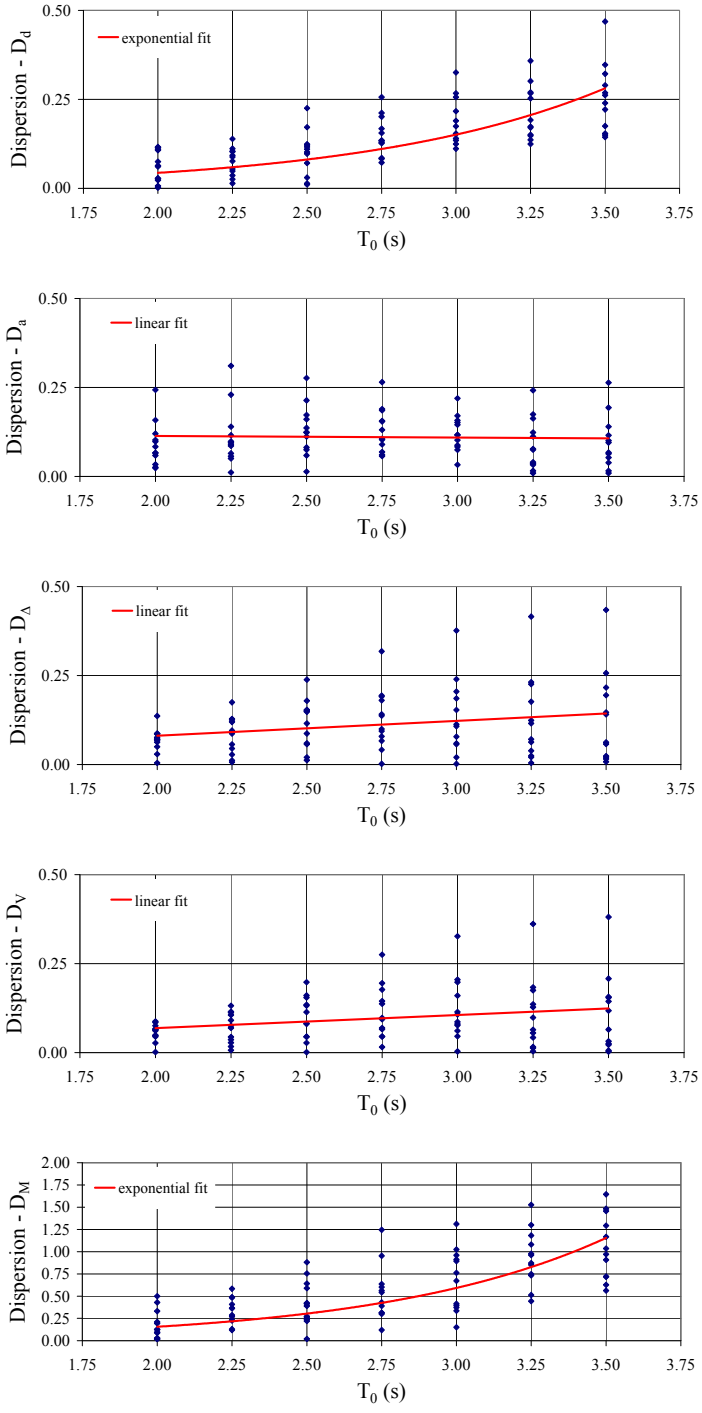

Fig. 11 Variation of dispersion calculated using peak base displacement (D_d), peak top floor acceleration (D_a), peak first story drift (D_Δ), peak base shear (D_V), and peak torsional base moment (D_M) with respect to the rigid-body-mode period, T_0

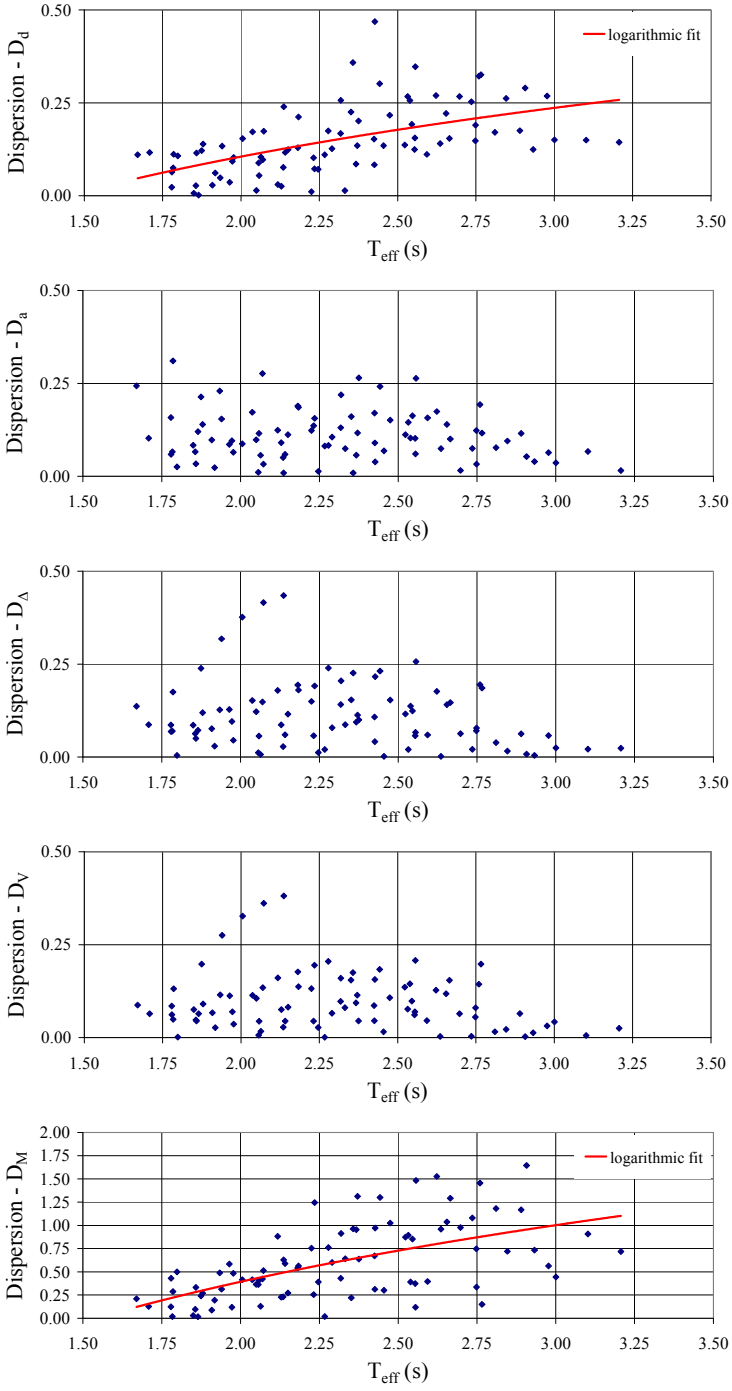

Fig. 12 Variation of dispersion calculated using peak base displacement (D_d), peak top floor acceleration (D_a), peak first story drift (D_Δ), peak base shear (D_V), and peak torsional base moment (D_M) with respect to the effective period, Teff

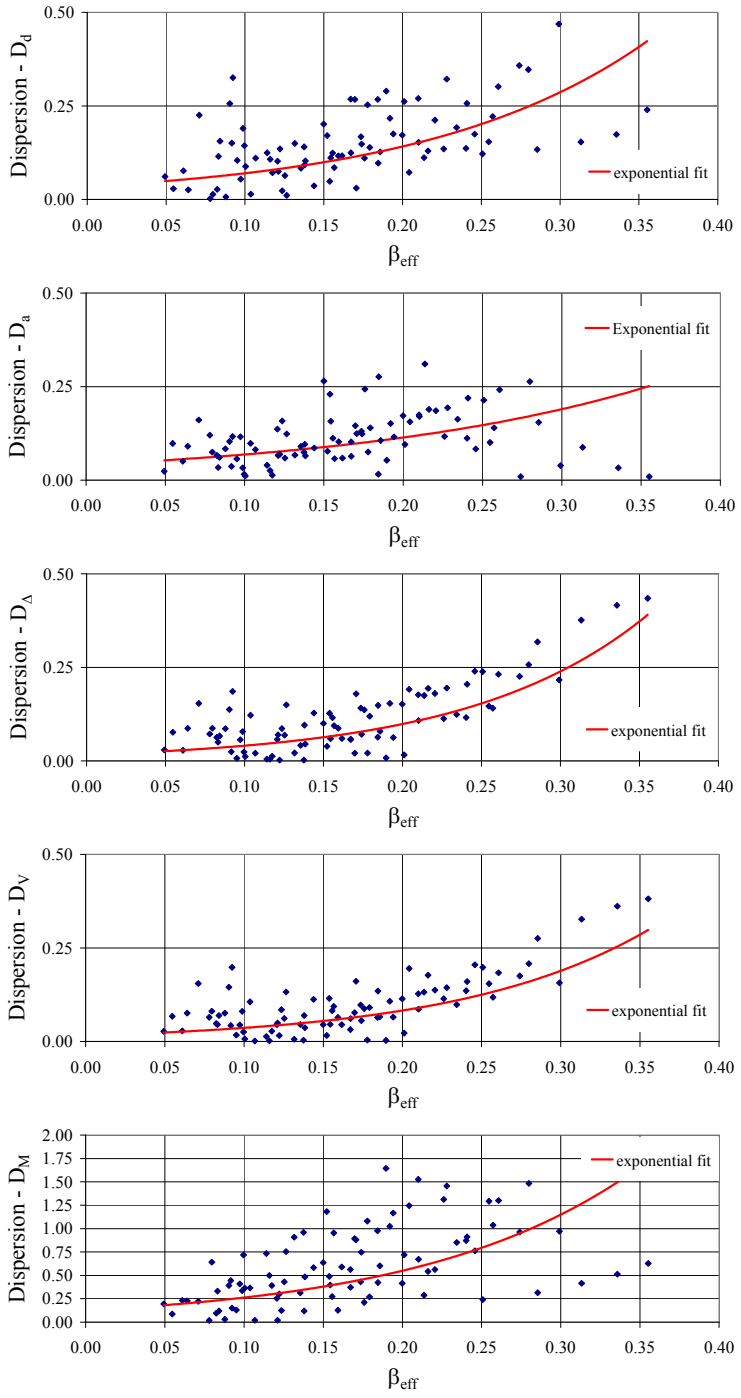

Fig. 13 Variation of dispersion calculated using peak base displacement (D_d), peak top floor acceleration (D_a), peak first story drift (D_Δ), peak base shear (D_V), and peak torsional base moment (D_M) with respect to the effective viscous damping ratio, β_{eff}

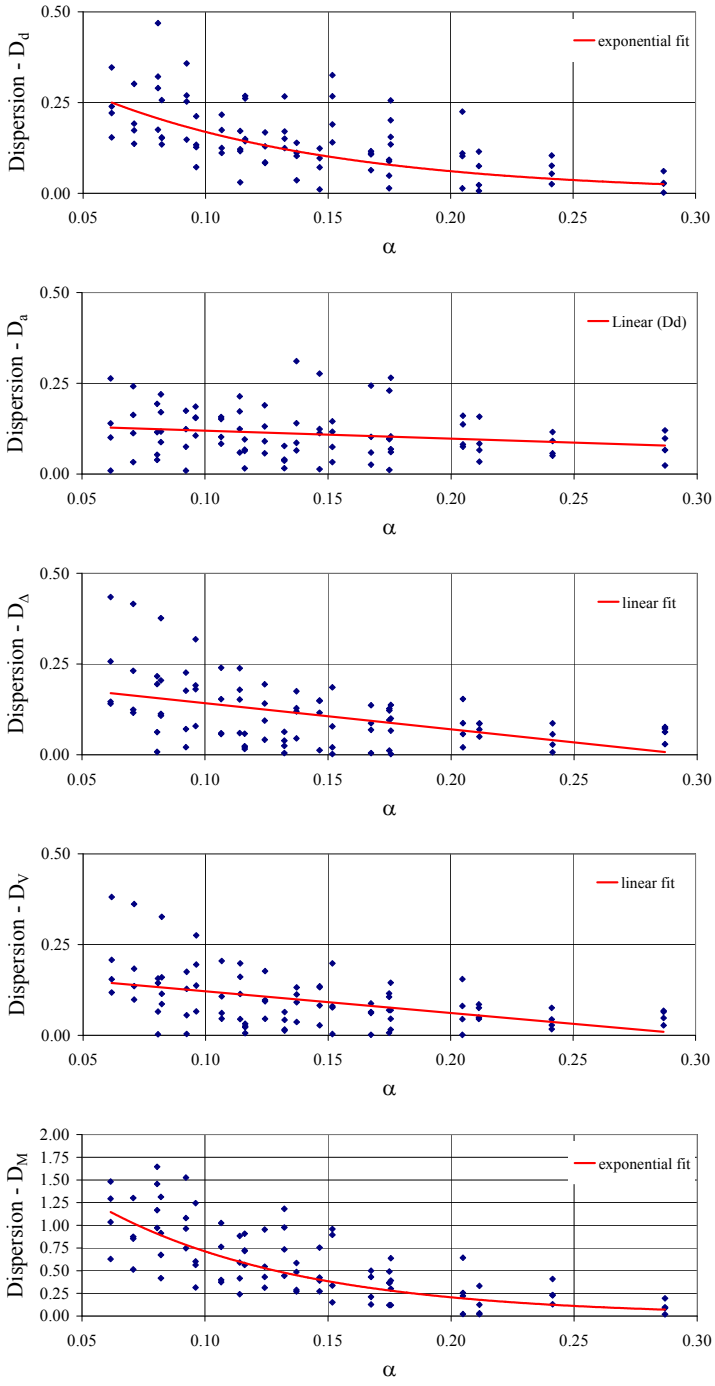

Fig. 14 Variation of dispersion calculated using peak base displacement (D_d), peak top floor acceleration (D_a), peak first story drift (D_Δ), peak base shear (D_V), and peak torsional base moment (D_M) with respect to the post-yield to the pre-yield stiffness ratio, α

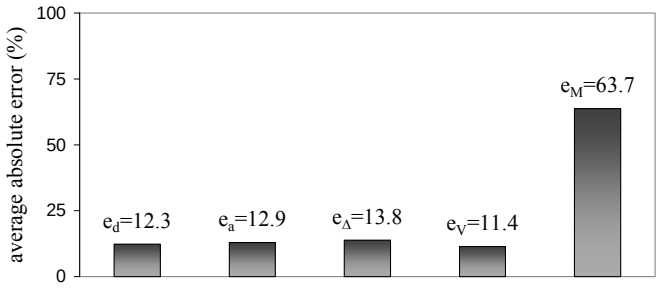

Fig. 15 Average absolute errors in peak structural responses arising from equivalent linear modeling of actual nonlinear isolation system models

6. Conclusions

In order to be able to use the seismic analysis methods for seismic-isolated structures which are based on linear elastic theory, the seismic isolators, which essentially exhibit nonlinear hysteretic behavior, have to be defined as equivalent linear elements with effective stiffness and effective viscous damping properties. However, equivalent linear modeling and analysis may lead to significant errors in the peak seismic response terms of multi-story structures. In an effort to shed light to this issue, generic five story three dimensional shear structure models equipped with nonlinear isolation systems of different characteristics and their equivalent linear counterparts are subjected to historical near-fault earthquakes and peak seismic response terms such as isolation system displacements, top floor accelerations, first story drifts, base shears and torsional base moments are evaluated and compared. Based on the results obtained in this study, following conclusions are reached:

1. Equivalent linear models produce better estimates of peak base displacements and peak torsional base moments for seismic-isolation systems with smaller effective periods and for those with smaller rigid-body mode periods. There exists no clear relation between the effective period or the rigid-body mode period and the accuracy of the estimates of other response parameters.
2. Equivalent linear models produce much better estimates of all structural response parameters -i.e peak base displacements, peak top floor accelerations, peak first story drift ratios, peak base shears, and peak torsional base moments- for seismic-isolation systems with smaller effective viscous damping ratios and for those with bigger post-yield to pre-yield stiffness ratios.
3. While equivalent linear modeling produces unconservative estimates of peak base displacements and peak torsional base moments, it produces conservative estimates of peak top floor accelerations, peak first story drift ratios, and peak base shears. Especially, the estimates of peak torsional base moments in eccentric cases can be highly unconservative, which would cause safety risks particularly for the isolators and the columns which are located close to the corners of seismically isolated structures.
4. The efficacy of equivalent linear modeling in predicting seismic responses of seismically isolated buildings is affected by bidirectional loading and biaxial interaction. Since the

biaxial interaction occurs at the isolation level, its effect is more prominent on the estimates of isolation system displacements and less on the estimates of other response parameters.

References

AASHTO (American Association of State Highway and Transportation Officials) (1999), *Guide Specifications for Seismic Isolation Design* Washington, D.C.

ASCE (2006), American Society of Civil Engineers, ASCE/SEI 7-05 *Minimum Design Loads for Buildings and Other Structures*, Virginia, USA.

Alhan, C. and Sürmeli, M. (2011), "Shear building representations of seismically isolated buildings", *Bull. Earthq. Eng*., **9**(5), 1643-1671.

Alhan, C. and Şahin, F. (2011), "Protecting vi bration-sensitive contents: an investigation of floor accelerations in seismically isolated buildings", *Bull. Earthq. Eng*., **9**(4), 1203-1226.

Cardone, D., Palermo, G. and Dolce, M. (2010), "Direct displacement-based design of buildings wih different seismic isolation systems", *J. Earthq. Eng*., **14**(2),163-191.

Chapra, S.C. and Raymond, C. (2002), *Numerical Methods for Engineers: With software and programming applications*, New York (NY), McGraw-Hill.

Dall'Asta, A. and Ragni, L. (2008), "Dynamic systems with high damping rubber: Nonlinear behavior and linear approximation", *Earthq. Eng. Struct. D*., **37**(13), 1511-1526.

Dicleli, M. and Buddaram, S. (2006), "Improved effective damping equation for equivalent linear analysis of seismic-isolated bridges", *Earthq. Spectra*, **22**(1), 29-46.

Dicleli, M. and Buddaram, S. (2007a), "Equivalent linear analysis of seismic-isolated bridges subjected to near-fault ground motions with forward rupture directivity effect", *Eng. Struct*., **29**(1), 21-32.

Dicleli, M. Buddaram, S. (2007b), "Comprehensive evaluation of equivalent linear analysis method for seismic-isolated structures represented by sdof systems", *Eng. Struct*., **29**(8), 1653-1663.

Franchin, P., Monti, G. and Pinto, P.E. (2001), "On the accuracy of simplified methods for the analysis of isolated bridges", *Earthq. Eng. Struct. D*., **30**(3), 363-382.

Gueguen, P. (2012), "Experimental analysis of the seismic response of one base-isolation building according to different levels of shaking: example of the Martinique earthquake (2007/1129) Mw 7.3", *Bull. Earthq. Eng.*, **10**(4), 1285-1298.

Heaton, T.H., Hall, J.F., Wald, D.J. and Halling, M.W. (1995), "Response of high-rise and base-isolated buildings to a hypothetical Mw 7.0 blind trust earthquake", *Science*, **267**, 206-211.

Hwang, J.S. (1996), "Evaluation of equivalent linear analysis methods of bridge isolation", *J. Struct. Eng. -ASCE*, **122**(8), 972-976.

Hwang, J.S. and Chiou, J.M. (1996), "An equivalent linear model of lead-rubber seismic isolation bearings", *Eng. Struct*., **18**(7), 528-536.

Hwang, J.S. and Sheng, L.H. (1993), "Effective stiffness and equivalent damping of base-isolated bridges", *J. Struct. Eng.- ASCE*, **119**(10), 3094-3101.

Hwang, J.S. and Sheng, L.H. (1994), "Equivalent elastic seismic analysis of base-isolated bridges with lead-rubber bearings", *Eng. Struct*., **16**(3), 201-209.

Hwang, J.S., Sheng, L.H., and Gates, J.H. (1994), "Practical analysis of bridges on isolation bearings with bi-linear hystresis characteristics", *Earthq. Spectra*, **10**(4), 705-727.

ICBO (1997), International Conference Building Officials, *Uniform Building Code*, Volume 2: Structural Engineering Provisions. Whitties, CA, USA.

Jara, M. and Casas, J.R. (2006), "A direct displacement-based method for the seismic design of bridges on bi-linear isolation devices", *Eng. Struct*., **28**(6), 869-879.

Kalkan, E. and Kunnath, S.K. (2006) "Effect of fling step and forward directivity on seismic response of buildings", *Earthq. Spectra*, **22**(2), 367-390.

Kelly, J. (1999), "The role of damping in seismic isolation", *Earthq. Eng. Struct. D*., **28**(1), 3-20.

Kottegodai, N.T. and Rosso R. (1997), *Statistics, Probability and Reliability for Civil and Environmental Engineers*, New York (NY), McGraw Hill.

Lakshmanan, N., Kumar, K.S., Sreekala, R., Muthumani, K., Guru, J. and Gopalakrishnan, N. (2008), "Experimental investigations on the seismic response of a base-isolated reinforced concrete frame model", *J. Perform. Constr. Fac.*, **22**(5), 289-296.

Liu, J.L. (2005), "Exact solution of nonlinear hysteretic responses using complex mode superposition method and its application to base-isolated structures", *J. Eng. Mech. -ASCE*, **131**(3), 282-289.

Marioni, A. (2009), "Seismic retrofitting of three important buildings in Italy and Turkey", *Proceedings of ATC and SEI Conference on Improving the Seismic Performance of Existing Buildings and Other Structures*, pg 892-904, San Francisco, CA, USA, 9-11 December.

Matsagar, V.A. and Jangid, R.S. (2004), "Influence of isolator characteristics on the response of base-isolated structures", *Eng. Struct*., **26**(12), 1735-1749.

Naeim, F. and Kelly, J.M. (1999), *Design of seismic isolated structures: From theory to practice*, John Wiley & Sons, New York.

Nagarajaiah, S., Reinhorn, A.M. and Constantinou, M.C. (1991), *3D-Basis: Nonlinear dynamic analysis of three-dimensional base isolated structures: Part II*, Techical Report NCEER-91-0005, National Center for Earthquake Engineering, State University of New York at Buffalo.

Nagarajaiah, S. and Xiaohong, S. (2000), "Response of base-isolated USC Hospital Building in Northridge Earthquake", *J. Struct. Eng.- ASCE*, **126**(10), 1177-1186.

Pan, P., Zamfirescu, D., Nakashima, M., Nakayasu, N. and Kashiwa, H. (2005), "Base-isolation design practice in Japan: Introduction to the Post-Kobe approach", *J. Earthq. Eng*., **9**(1), 147-171.

PEER (2000), *Peer Strong Motion Databank*, University of California, Berkeley.
http://peer.berkeley.edu/smcat/search.html. Accessed 15 November 2009.

Özgür, M. (2010), *A comparison of seismic performances of linear and non-linear isolation systems*, *MSc Thesis*, Department of Civil Engineering, Institute of Science, Istanbul University (in Turkish).

Sarrazin, M., Moroni, O. and Roesset, J.M. (2005), "Evaluation of dynamic response characteristics of seismically isolated bridges in Chile", *Earthq. Eng. Struct. D*., **34**(4-5), 425-448.

Sayani, P. and Ryan, K. (2009), "Evaluation of approaches to characterize seismic isolation system s for design", *J. Earthq. Eng*., **13**(6), 835-851.

Tsai, C.S., Lin Y., Chen, W. and Su, H.C. (2010), "Tri-directional shaking table tests of vibration sensitive equipment with static dynamics interchangeable-ball pendulum system", *Earthq. Eng. Eng*. *Vib*., **9**(1), 103-112.

Turkington, D.H., Carr, A.J., Cooke, N. and Moss, P.J. (1989a), "Design methods for bridges on lead-rubber bearings", *J. Struct. Eng.- ASCE*, **115**(12), 3017-30030.

Turkington, D.H., Carr, A.J., Cooke, N. and Moss, P.J. (1989b), "Seismic design of bridges on lead-rubber bearings", *J. Struct. Eng. -ASCE*, **115**(12), 3000-30016.

York, K. and Ryan, K.L. (2008), "Distribution of lateral forces in base-isolated buildings considering isolation system nonlinearity", *J. Earthq. Eng*., **12**(7), 1185-1204.

FC